APPLYING ATMOSPHRIC MOISTURE TO IMPROVE RAINFALL ESTIMATION DURING HURRICANES

Peng Jia[*1] and Jie Wu[2]
[1]Graduate Student, Department of Geography, University of Florida
Gainesville, FL 32611, U.S.; Tel: +00-1-352-2818418;
Email: jiapengff@hotmail.com

[2]Institute of Remote Sensing Applications Chinese Academy of Sciences,
20, Datun Road, Chaoyang District, Beijing 100101; Tel: + 86-10-64889542;
E-mail: wujie@irsa.ac.cn

KEY WORDS: Atmospheric moisture, rainfall, hurricane, GIS, Kriging

ABSTRACT: The study used atmospheric moisture and rainfall history, combined with maximum wind speed, to improve the estimation of the rainfall caused by hurricanes**.** GIS, Kriging method and multi-variable regression analysis were primarily employed. The results are greatly instructive to both forecast the rainfall and protect people away from the potential flooding areas.

1. INTRODUCTION

Hurricanes may bring rainfall that can lead to flooding (Tootle et al 2005), which leads to the most death associated with hurricanes (Elsberry 2002), so the accurate rainfall forecasts remain a critical problem for reducing the damages brought by hurricanes. In the Rainfall Climatology and Persistence model (R-CLIPER) utilized operationally in the Atlantic Ocean basin by the National Hurricane Center (NHC) for hurricane rainfall forecasts, the storm intensity is considered as the major factor (Jiang et al 2008a). After that, the effects of vertical wind shear and topography are taken into account and combined with the effects modeled in R-CLIPER in a new model called the Parametric Hurricane Rainfall Model (PHRaM) (Lonfat et al 2007). The maximum accumulated rainfall over land, as the function of satellite-derived rainfall potential over ocean prior to landfall, storm size and translation speed, has also been studied and the high correlation has been found (Jiang et al 2008b).

In addition to the storm inherent features, environmental parameters are also crucial to affect the rainfall, such as moisture budget (Carr and Bosart 1978; DiMego and Bosart 1982), total precipitable water (Rodgers and Pierce 1995, in Jiang et al 2008a), horizontal moisture convergence (Jiang et al 2008c and 2008d) and ocean surface flux (Jiang et al 2008a). However, few statistical relationships between rainfall and environmental moisture during hurricanes have been documented (Jiang et al 2008a). It has also been found that (Jiang et al 2008a) before the landfall of hurricanes, a stronger statistical relationship existed between accumulated rainfall and maximum wind intensity than after landfall, that is, the correlation between rainfall and maximum wind over ocean (pre-landfall) was stronger than over land (post-landfall) during hurricanes. The similar stronger correlations have also been found between the same dependent variable (accumulated rainfall) and other independent variables including precipitable water (PWAT), horizontal moisture convergence (HMC) and ocean surface flux (OSF). The environmental moisture data, in the study above, was interpolated into 3-hourly from 12-hourly temporal resolution with 111×111 km^2 spatial resolution. Also, It has been documented that there was a great improvement for describing the accumulated rainfall after combining PWAT, HMC and OSF with maximum wind speed; however, there were no pronounced distinctions between only adding PWAT and adding all of three, which would make the prediction more practical and greatly reduce the prediction error because HMC and OSF were model-derived parameters instead of being easily from satellite-derived observations.

Based on author's current literature review, no quantitative relationship between accumulated rainfall and atmospheric moisture has been studied for short-term forecast purposes. This study attempted to fill this gap by 1) using time lags to adjust the correlations between moisture and rainfall for short-term forecast purposes and 2) utilizing the moisture and rainfall data with higher temporal resolution to aid the maximum wind speed predicting the rainfall brought by hurricanes.

Precipitable Water (PWAT) is the depth of liquid water that would result after precipitating all of the water vapor in a vertical column over a given location. In this study it was employed to represent the atmospheric moisture. AR stands for the accumulated rainfall on the ground. The maximum wind speed is the total velocity gauged at the landfall of hurricanes, which is synthesized by the speed of moving forward and spinning within the storm.

Spatial statistics and Geographic Information System (GIS), while different, rely on each other in important ways. GIS software can be used to create covariates for inclusion in statistical models and to visualize the output from statistical models. Spatial statistics provides modeling and inference techniques for drawing conclusions from geographical data and provides a group of methods for spatial smoothing and accounting for non-spatial covariates in estimating spatial surfaces. In this study, we focused our attention on predicting the average and total accumulated rainfall because they are more stable and easier to predict than maximum and minimum ones. The latter two need accurate locations where they may occur to make themselves more practical.

2. DATA

2.1 Study Cases & Storm Records

In this study we examined three hurricanes making their landfalls over the southeastern continent of U.S. in September 2004, named Frances, Ivan and Jeanne. Frances made its first landfall over the southern end of Hutchinson Island near Stuart in the state of Florida at about 0430 UTC on 5th September as a Category 2 hurricane (90 knot), according to the Saffir-Simpson Intensity Scale; then it moved northwestward and emerged into the northeastern Gulf of Mexico near early on 6th, followed by the second landfall near the mouth of the Aucilla River in the Florida Big Bend region at about 1800 UTC on 6th at a wind speed of 90 knot. Ivan made the first landfall as a Category 3 hurricane (105 knot) at approximately 0650 UTC on 16th over the west of Gulf Shores in Alabama state, near the border between southern Alabama and western Florida; after landfall, it kept moving towards northeast across Alabama, along the border of Tennessee and North Carolina, then across Virginia and went into Atlantic from Delmarva peninsula in Virginia where it became an extra-tropical low around 1800 UTC on 18th; over the next 3 days, it moved south and southwestward over Atlantic and made its second landfall over Fort Lauderdale in Florida from Atlantic near the morning of 21st at a rate of 25 knot and eventually emerged over the southeastern Gulf of Mexico later that afternoon. Jeanne, which has similar features as Frances, e.g. landfall location (Hutchinson Island near Stuart, Florida), minimum central pressures (960 mb for Frances and 950 mb for Jeanne) and tracks of movement (crossing the coastline northwestward at about 280°), made its only landfall near 0400 UTC on 26th September at about 105 knot, and moved across central Florida, Tampa and central Georgia over the next 36 hours, then continued moving northwards. We derived the spatial locations of three storm centers and the maximum wind speed in 6-hourly increments from HURDAT (NHC 2006) and utilized the extended best track data (Demuth et al 2006) to estimate storm size.

2.2 Rainfall & Moisture Data

In this study, what we did was for future prediction instead of real-time forecast, so we selected 3-hourly Tropical Rainfall Measuring Mission (TRMM) and Other Rainfall Estimate (3B42 V6) with 32.2×32.1 km^2 spatial resolution as the accumulated rainfall estimates instead of Real-time TRMM product on which several simplifications were imposed for realizing real-time effect. It is a combined product based on two different sets of sensors: Microwave and IR (Huffman et al. 2007, in Jiang et al 2008a). In the current TRMM 3B42 system, passive microwave observations from TMI, AMSR-E and SSM/I are converted to precipitation estimates with sensor-specific versions of the Goddard Profiling Algorithm (GPROF) (Kummerow et al 1996, in Jiang et al 2008a). For the measurements over land and ocean, GPROF selected different channels and strategies, which leads to about 17% positive biases over land, compared with rain gauge data, and 9% negative biases over ocean (Jiang et al 2008a). We derived precipitable water (PWAT) data in 3-hourly increments with 21.4×27.8 km^2 spatial resolution from the North American Regional Reanalysis (NARR) dataset, which provides higher temporal and spatial resolution than the ones calculated from the Navy Operational Global Atmospheric Prediction System (NOGAPS) analysis with 12-hourly temporal resolution and 111×111 km^2 spatial resolution.

3. METHODS

3.1 Kriging

Kriging is a group of geostatistical techniques to interpolate a certain kind of values at unobserved locations base on their observed counterparts at nearby locations, which could minimize the estimation error and produce a continuous and smooth surface from some discrete points. A typical geostatistical routine might interpolate the value for a given location using several nearest neighbor values weighted by distance and the degree of autocorrelation present for that distance. The quality of interpolated values depends on the spatial continuity of the phenomenon and the distribution of separate known points. Both PWAT and AR dataset we used in this study contain evenly-distributed gridded data; in addition, both atmospheric moisture and precipitation are typical continuous phenomenon. Therefore, Kriging is a good choice to interpolate these two kinds of data. We selected Ordinary Kriging and Spherical semivariogram model in this study (Figure 2).

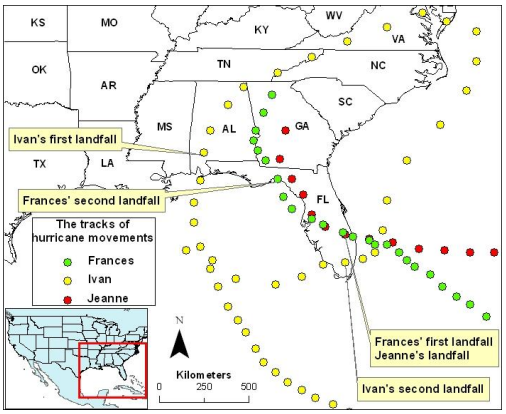

Figure 1 Tracks of movement of three hurricanes

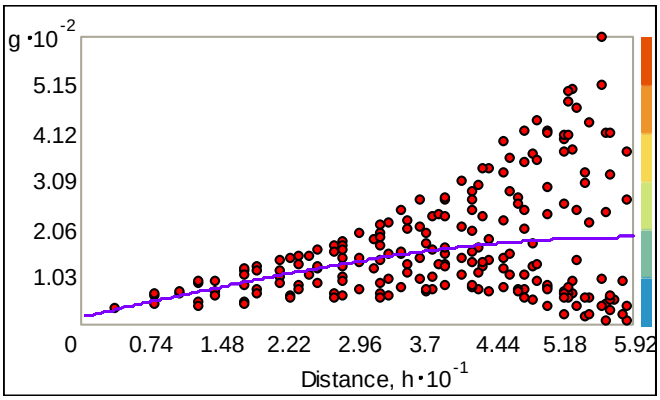

Figure 2 Semivariogram with Spherical model

3.2 Regression Analysis

Regression analysis is a major tool to make a forecast based on past and current trends and historical empirical evidence. It is used to model the relationship between a dependent variable and one or more independent variables in order to assess the extent to which a dependent variable are affected by one explanatory variable (Bivariate) or a combination of independent variables (Multivariate). Stepwise regression employs a screening procedure to determine which explanatory variables are retained and dropped from the model based on their explanatory power by setting a certain threshold of Probability or F-statistic. It is a sequential method for adding and removing regressors to determine a final regression model which provides the best possible fit. There are four types of stepwise procedures: Forward Stepwise Regression (FSR), Backward Stepwise Regression (BSR), General Stepwise Regression (GSR) and Min. MSE Stepwise. Here we selected FSR, which starts with a full-blown model including all k regressors we are interested in. First, it will find the explanatory variable that explains the greatest amount of variation in the dependent variable; if its p-value is lower than the threshold we set up, it will be added into the model. Then, find the variable that provides the secondary greatest amount of explanatory power to the model based on the unexplained variation from the model and check the corresponding p-value. Repeat the process until no variables in the pool are qualified.

F-ratio, recorded as the ratio of explained variation to unexplained variation, is often used to assess the explanatory power provided by the independent variables. The p-value, corresponding to a computed F-ratio, tells us the percentage of the confidence level up to which we could reject the null hypothesis. In addition to F-ratio, we also employed adjusted R^2 (adjusted coefficient of determination) to assess the overall strength of our regression models which supersedes its unadjusted version R^2 (coefficient of determination) which might increase just due to chance. Maximizing Adjusted R^2, which will keep approaching 1.0 with F-ratio increasing, is one goal of improving regression models and it is easier to assess than F-ratio.

The assumption of normality of error plays a critical role in assessing the structure and significance of our regression models because Non-normality of error may inflate the standard error, which leads us to fail to reject some null hypothesis that should be rejected. Therefore, we used a combination of Kolmogorov-Smirnov, Shapiro-Wilk and Anderson-Darling test to test the normality of error. Kolmogorov-Smirnov test is often used for testing whether the current group of samples comes from a completely specified continuous distribution; Shapiro-Wilk test is popular because it is valid for samples the number of which ranges from 3 to 5000; Anderson-Darling test is useful especially when the number of samples is less than 25 or 40 because a large sample size may reject the assumption of normality with only slight imperfections, but industrial data with sample sizes of 200 and more have passed the Anderson–Darling test, so here we used it to assist other tests with caution.

3.3 Radius Selection

The forecast wind radii are the farthest extent from the center of 34-, 50-, and 64-knot winds in each quadrant of a tropical cyclone expected for each forecast period. Although not an exact representation of the expected wind field, they are intended to show the expected size of the storms and the areas potentially affected by sustained winds of 34 knot (tropical storm force), 50 knot and 64 knot (hurricane force) from a tropical cyclone. Therefore, not all locations within the forecast wind radii will necessarily experience the indicated wind speeds. About 230 km is often regarded as the average radius of the rain fields at landfall (Matyas 2010). Based on the average radius and forecast wind radii of three hurricanes at landfall (Table 1), we took 111 km as the radius of inner cores of hurricanes and 333 km as the environment around the storm centers, for the purpose of observing if significant correlations exist between accumulated rainfall and precipitable water within these two levels of radius.

Hurricane	34-knot (km)	50-knot (km)	64-knot (km)
Frances first landfall	231.5 - 324.1	138.9 - 231.5	74.08 - 138.9
Frances second landfall	0 - 166.68	0 - 46.3	0
Ivan first landfall	138.9 - 463	74.08 – 231.5	46.3 – 83.34
Ivan second landfall	0	0	0
Jeanne landfall	231.5 – 333.36	111.12 – 185.2	74.08 – 111.12

Table 1 Radii of three hurricanes, each pair of values representing the range (minimum - maximum) of forecast wind radii in four quadrants at a given wind speed

3.4 Variable Selection

The precipitable water in the air needs a couple of hours or days to drop onto the ground, so to consider time lags between PWAT and AR data is crucial for forecast purposes. It has been found that although better than the results in which the maximum wind speed was mainly used to predict the rainfall, the 12-h time lag provided almost the same correlation coefficients for land (0.60), ocean (0.64) and all conditions (0.66) as their counterparts without considering any time lag, and the 24-h time lag even provided slightly smaller ones for land (0.56), ocean (0.60) and all conditions (0.63) (Jiang et al 2008a). In this study, we regarded the buffer zones around all the storm centers occurring within 72 hours centered at landfall time as our study areas. The records of storm centers are available every six hours (0000, 0600, 1200 and 1800 UTC), and each center corresponds to both an inner area and an outer environment area around it; therefore, 13 storm centers for each landfall of each hurricane should, theoretically, be selected, but as some time points around two times of Frances' landfall are overlapping, so 19 centers for Frances, 26 for Ivan and 13 for Jeanne, 19 centers of Frances were selected, that is, 58 inner areas and 58 outer ones totally for our study. Within each study area, in addition to the PWAT and AR at the time when landfall occurred, we also calculated the PWAT and AR values 3 and 6 hours prior to landfall, and the ones 3 and 6 hours after landfall, respectively. For clearer explanations, we defined all the variables for the storm center at a given time in Table 2.

Variable	Definition
B6_PWAT(AR)_AVG(SUM)	The average(total) PWAT(AR) within a circle of 111 km radius centered at the location at which the storm center would arrive after 6 hours
B3_PWAT(AR)_AVG(SUM)	The average(total) PWAT(AR) within a circle of 111 km radius centered at the location at which the storm center would arrive after 3 hours
PWAT(AR)_AVG(SUM)	The average(total) PWAT(AR) within a circle of 111 km radius centered at the storm center at landfall
A3_PWAT(AR)_AVG(SUM)	The average(total) PWAT(AR) within a circle of 111 km radius centered at the location where the storm center had left for 3 hours
A6_PWAT(AR)_AVG(SUM)	The average(total) PWAT(AR) within a circle of 111 km radius centered at the location where the storm center had left for 6 hours
PWAT(AR)_AVG(SUM)3	The average(total) PWAT(AR) within a circle of 333 km radius centered at the storm center at landfall
B6(B3/A3/A6)_PWAT(AR)_ AVG(SUM)3	(The same meanings as above, just the radius was changed from 111 to 333 km)

Table 2 Definitions of all the variables involved in the regression analysis

4 Results

4.1 Maximum wind speed

At first, we only used maximum wind speed at landfall to explain the rainfall at landfall within both inner and outer areas and predict the rainfall brought by hurricanes within the same two areas after 3 hours and 6 hours, respectively. The results were shown in Table 3(Sp. stands for the number of samples, the same in Table 4 and 5).

4.2 Maximum wind speed, PWAT and Rainfall history

We used precipitable water and rainfall history data to aid the maximum wind speed to see if there were some improvements to explain the rainfall brought by hurricanes. The results were shown in Table 4 and Table 5.

5. CONCLUSIONS

In Table 3, all of the coefficients are positive, which means the higher the maximum wind speed is, the more rainfall the hurricane could bring both at and after the landfall. In the inner area, in addition to explain the rainfall at

the same time, the maximum wind speed of hurricanes at landfall also provided good predictions, to some extent, for the average and total rainfall at the locations where it left 3 to 6 hours ago. However, by the comparison of adjusted R^2, the introduction of precipitable water and rainfall history data did improve the ability of predicting. All of our dependent variables were better explained (AR_Avg: 0.857 to 0.909; A3_AR_Avg: 0.799 to 0.897; A3_AR_Sum: 0.820 to 0.879; A6_AR_Avg: 0.772 to 0.831; A6_AR_Sum: 0.856 to 0.930) except the total amount of rainfall at landfall (AR_Sum: 0.850 to 0.787).

It was proved that, at the time of landfall, the average rainfall in the inner area of the storm center was influenced by both the maximum wind speed at that time and the atmospheric moisture and rainfall before 3 hours; it was a little hard to know the total rainfall at landfall as the measurable variables before the landfall did not improve its estimation. After 3 hours, away from the landfall, both the average and total rainfall within the same area were better estimated by the total rainfall at landfall, the true amount of which, although hard to predict before the landfall, could be gauged by satellite in the real time of landfall and was hence greatly helpful. After another 3 hours passed, it was still the maximum wind speed at landfall combined with the atmospheric moisture and rainfall 3 hours ago that estimated the average rainfall better than only maximum wind speed. The total rainfall, shown in the model, was greatly influenced by the atmospheric moisture and maximum wind speed at the time of landfall, that is, 6 hours ago, the underlying physical correlation of which needed further meteorological study, but we could, at least, see the importance of the atmospheric moisture.

When the hurricane makes landfall, people living there can be effectively evacuated or protected based on the prediction of the storm centers in advance, which is becoming more and more accurate; however, with the center of the hurricane moving away and people starting to go back, the real danger caused by following rainfall is approaching. The results are of great importance to the people and regions that will come across the hurricanes in future.

Variable	Constant included	Sp.	R^2	F-ratio	K-S test	S-W test	A-D test
AR_Avg	YES	*56*	*0.783*	*199.150*	*0.123*	*0.410*	*>0.15*
	NO	**57**	**0.857**	**336.550**	**0.004**	**0.002**	**<0.01**
AR_Sum	YES	57	0.756	174.103	0.215	0.610	>0.15
	NO	**58**	**0.850**	**323.809**	**0.002**	**0.000**	**<0.01**
A3_AR_Avg	YES	58	0.693	129.819	0.001	0.003	<0.01
	NO	**58**	**0.799**	**227.286**	**0.000**	**0.000**	**<0.01**
A3_AR_Sum	YES	54	0.699	123.913	0.018	0.005	<0.01
	NO	**54**	**0.820**	**240.966**	**0.002**	**0.000**	**<0.01**
A6_AR_Avg	YES	52	0.730	139.167	0.029	0.011	<0.01
	NO	**53**	**0.772**	**175.867**	**0.000**	**0.000**	**<0.01**
A6_AR_Sum	YES	**47**	**0.856**	**274.873**	**0.002**	**0.027**	**<0.01**
	NO	54	0.768	175.517	0.000	0.000	<0.01

Table 3 Estimations based on only wind speed (Bold showed the best) (Confidence level = 95%)

Dependent	Independent variable(s)	Sp.	R^2	F-ratio	K-S	S-W	A-D
AR_Avg	*Constant , B3_AR_Avg , KNOT*	*57*	*0.812*	*122.266*	*0.001*	*0.022*	*<0.01*
	B3_PWAT_Avg , B3_AR_Avg , KNOT	**57**	**0.909**	**186.098**	**0.001**	**0.041**	**<0.01**
	Constant , B3_AR_Sum , KNOT	56	0.804	113.978	0.001	0.009	<0.01
	B3_PWAT_Sum , B3_AR_Sum , KNOT	56	0.905	174.516	0.003	0.018	<0.01
	Constant , KNOT	*56*	*0.783*	*199.15*	*0.123*	*0.41*	*>0.15*
	B3_PWAT_Avg3 , KNOT	*56*	*0.895*	*234.954*	*0.542*	*0.637*	*>0.15*
	B6_PWAT_Avg , KNOT	*56*	*0.897*	*240.722*	*0.417*	*0.649*	*>0.15*
	B6_PWAT_Sum3 , KNOT	*56*	*0.897*	*239.812*	*0.14*	*0.365*	*>0.15*
AR_Sum	*Constant , B3_AR_Avg , KNOT*	*57*	*0.775*	*97.606*	*0.006*	*0.114*	*0.031*
	B3_PWAT_Avg , B3_AR_Avg , KNOT	*57*	*0.895*	*158.937*	*0.041*	*0.166*	*0.062*
	Constant , B3_AR_Sum , KNOT	**57**	**0.787**	**104.2**	**0.004**	**0.099**	**<0.01**
	B3_PWAT_Sum , B3_AR_Sum , KNOT	*57*	*0.901*	*170.139*	*0.031*	*0.131*	*0.015*
	Constant , KNOT	*57*	*0.756*	*174.103*	*0.215*	*0.601*	*>0.15*
	B3_PWAT_Avg3 , KNOT	*57*	*0.884*	*212.878*	*0.29*	*0.697*	*>0.15*
	B6_PWAT_Sum , KNOT	*57*	*0.890*	*227.319*	*0.214*	*0.611*	*>0.15*
	B6_PWAT_Avg3 , KNOT	*57*	*0.886*	*218.39*	*0.485*	*0.746*	*>0.15*

Table 4 Estimations based on PWAT, AR and wind speed (Bold showed the best) (Confidence level = 95%)

Dependent	Independent variable(s)	Sp.	R^2	F-ratio	K-S	S-W	A-D
A3_AR_Avg	PWAT_Avg , AR_Avg , KNOT	58	0.878	137.049	0.012	0.043	0.012
	AR_Sum	**57**	**0.897**	**488.963**	**0.009**	**0.022**	**<0.01**
	PWAT_Avg3 , KNOT	58	0.835	145.075	0.000	0.007	<0.01
	B3_PWAT_Sum , KNOT	58	0.839	149.119	0.016	0.008	<0.01
	B3_PWAT_Avg3 , KNOT	58	0.832	142.093	0.000	0.004	<0.01
A3_AR_Sum	AR_Avg , KNOT	58	0.831	140.264	0.000	0.000	<0.01
	Constant , PWAT_Sum , AR_Sum	*57*	*0.815*	*124.518*	*0.293*	*0.228*	*0.112*
	AR_Sum	**57**	**0.879**	**407.791**	**0.000**	**0.004**	**<0.01**
	B3_PWAT_Avg , KNOT	54	0.843	142.943	0.007	0.005	<0.01
	B3_PWAT_Sum , KNOT	54	0.851	151.371	0.017	0.012	<0.01
A6_AR_Avg	A3_PWAT_Avg , A3_AR_Avg , KNOT	*50*	*0.916*	*178.12*	*0.042*	*0.094*	*0.013*
	Constant , A3_AR_Sum , KNOT	56	0.723	72.67	0.000	0.000	<0.01
	A3_PWAT_Sum , A3_AR_Sum , KNOT	**56**	**0.831**	**91.133**	**0.001**	**0.001**	**<0.01**
	PWAT_Avg , KNOT	*49*	*0.896*	*207.467*	*0.092*	*0.043*	*0.011*
	PWAT_Sum , KNOT	*53*	*0.839*	*136.474*	*0.111*	*0.124*	*0.034*
A6_AR_Sum	A3_PWAT_Avg , A3_AR_Avg , KNOT	*50*	*0.924*	*198.894*	*0.071*	*0.039*	*<0.01*
	Constant , A3_AR_Sum , KNOT	*50*	*0.855*	*145.105*	*0.154*	*0.432*	*0.14*
	A3_PWAT_Sum , A3_AR_Sum , KNOT	*50*	*0.914*	*173.917*	*0.237*	*0.442*	*>0.15*
	PWAT_Avg , KNOT	**47**	**0.93**	**306.156**	**0.000**	**0.029**	**<0.01**
	PWAT_Sum , KNOT	53	0.837	133.812	0.000	0.004	<0.01

Table 5 Estimations based on PWAT, AR and wind speed (Bold showed the best) (Confidence level = 95%)

6. LIMITATIONS

The limited numbers of the hurricanes and influencing variables are included and maybe not representative enough. Some outer error may come from the satellite-derived data and Kriging interpolation. In future, we will continue expanding our sample pool and consider more variables for more accurate predictions.

7. REFERENCES

Tootle, G., Mirti, T. and T. Piechota. 2005. Technical Notes: Magnitude and return period of 2004 hurricane rainfall in Florida. Journal of Floodplain Management 5: 32-37.

R. L. Elsberry. 2002. Predicting Hurricane Landfall Precipitation: Optimistic and Pessimistic Views from the Symposium on Precipitation Extremes. Bulletin of the American Meteorological Society 83(9): 1333-1340.

Jiang, H., Halverson, J.B. and E.J. Zipser. 2008a. Influence of environmental moisture on TRMM-derived tropical cyclone precipitation over land and ocean. Geophysical Research Letters 35, L17806, doi: 10.1029/2008GL034658.

Lonfat, M., Rogers, R., Marchok, T. and F. D. Marks Jr. 2007. A parametric model for predicting hurricane rainfall. Monthly Weather Review 135: 3086–3097.

Jiang, H., Halverson, J. B., Simpson, J. and E. J. Zipser. 2008b. Hurricane "Rainfall Potential" derived from satellite observations aids overland rainfall prediction. Journal of Applied Meteorology and Climatology 47: 944-959.

Carr, F. H. and L. F. Bosart. 1978. A diagnostic evaluation of rainfall predictability for tropical storm Agnes, June 1972. Monthly Weather Review 106: 363–374.

DiMego, G. J. and L. F. Bosart. 1982. The transformation of Tropical Storm Agnes into an extratropical cyclone. Part II: Moisture, vorticity and kinetic energy budgets. Monthly Weather Review 110: 412–433.

Jiang, H., Halverson, J. B. and J. Simpson. 2008c. On the differences in storm rainfall from Hurricanes Isidore and Lili. Part I: Satellite observations and rain potential. Weather Forecasting 23: 44– 61.

Jiang, H., Halverson, J. B., Simpson, J. and E. J. Zipser. 2008d. On the differences in storm rainfall from Hurricanes Isidore and Lili. Part II: Water budget. Weather Forecasting 23: 29–43.

NHC. 2006. Official Record of Hurricanes and Tropical Storms in the Atlantic Basin. Available at www.aoml.noaa.gov/hrd/Data_Storm.html.

Demuth, J. L., DeMaria, M. and J. A. Knaff. 2006. Improvement of advanced microwave sounding unit tropical cyclone intensity and size estimation algorithms. Journal of Applied Meteorology and Climatology 45: 1573-1581.

C.J. Matyas. 2010. Use of Ground-based Radar for Climate-Scale Studies of Weather and Rainfall. Geography Compass 4(9): 1218-1237.